

Supporting Information

Bis-indole/carbazole based C5-Curcuminoid fluorescent probe with large Stokes shift for selective detection of biothiol and application to live cell imaging

Pinaki Bhattacharjee,^a Sourav Chatterjee,^a Anushree Achari,^a Abhijit Saha,^b Debkumar Nandi,^a Chiranjit Acharya,^a Kasturi Chatterjee,^c Surajit Ghosh,^b Snehasikta Swarnakar,^c and Parasuraman Jaisankar^{a,*}

^aLaboratory of Catalysis and Chemical Biology, Organic and Medicinal Chemistry Division, CSIR-Indian Institute of Chemical Biology, 4 Raja S. C. Mullick Road, Kolkata - 700 032, India

^bChemistry-Biology Interface Laboratory, Organic and Medicinal Chemistry Division, CSIR-Indian Institute of Chemical Biology, 4 Raja S. C. Mullick Road, Kolkata - 700 032, India.

^cCancer Biology and Inflammatory Disorder Division, CSIR-Indian Institute of Chemical Biology, 4 Raja S. C. Mullick Road, Kolkata - 700 032, India.

Corresponding author e-mail: jaisankar@iicb.res.in

Table of Contents:

Section I:	General Information	S2
Section II:	Optimization and experimental procedure and for PJ1-PJ6	S3-S4
Section III:	Photophysical property studies of PJ1-PJ6	S5-S7
Section IV:	Determination of detection limit	S7-S8
Section V:	Kinetic study of the response of the probe PJ1 with Cys	S9
Section VI:	Determination of fluorescence quantum yield of PJ1	S9
Section VII:	Fluorescence decay profile of probe PJ1	S9
Section VIII:	Fluorescence quenching at different pH of PJ1	S9-S10
Section IX:	Photostability of PJ1 vs PJ5	S10
Section X:	Kinetics of sensing of PJ1 studied by HPLC	S11
Section XI:	Procedure for cell culture and fluorescence imaging	S11-S14
Section XII:	¹ H NMR, ¹³ C NMR, and FT-IR, HRMS spectra of PJ1-PJ6 and HPLC of PJ3	S15-S25
Section XIII:	Color change of PJ1 solution with incubated various amino acids	S25
Section XIV:	References	S26

Section I: General Information

All the reactions were carried out in oven-dried glassware. All reagents were purchased from commercial suppliers and used without further purification. Melting points were determined in open glass capillaries and are uncorrected. ^1H NMR spectra were recorded on a JEOL JNM-ECZ 400 MHz, and Bruker DRX 600 MHz NMR instrument at ambient temperature in CDCl_3 , $\text{DMSO}-d_6$ and Acetonitrile- d_3 . ^{13}C NMR spectra were recorded at 100 MHz, and 150 MHz at ambient temperature. The chemical shifts were recorded in parts per million (ppm) with TMS as internal reference. ^1H NMR is reported as follows: chemical shift, multiplicity (s=singlet, d=doublet, dd=doublet of doublets, t=triplet, q=quartet, m=multiplet), coupling constant and integration. Coupling constant (J) values are given in hertz (Hz). ^{13}C NMR spectra was recorded with complete proton decoupling. Mass spectral data correspond to ESIMS and are given in m/z unit. ESIMS was done on a Waters^(R)Micromass^(R) Q-TOF MicroTM Mass Spectrometer. Infrared (IR) spectra were recorded on a BRUKER FT-IR Model-TENSOR 27. Spectra were calibrated against the polystyrene absorption at 1601 cm^{-1} . Samples were scanned in neat or KBr discs. Analytical thin-layer chromatography (TLC) was carried out on Merck $20 \times 20\text{ cm}$ silica gel 60-F₂₅₄ plates. Column chromatography was done with Biotage flash, silica gel 100-200 mesh. Yields refer to quantities obtained after column chromatography. HPLC analyses were performed on a Shimadzu SPD-20A using PhenomenexLuna[®] C18 reverse phase column ($4.6\text{ mm} \times 250\text{ mm} \times 5\text{ }\mu\text{m}$) and Phenomenex Luna[®] $5\text{ }\mu\text{m}$ C18(2) 100 \AA , LC Column $250 \times 4.6\text{ mm}$. Reaction was carried in a microwave reactor (*Biotage Initiator microwave system EXP EU, part no. 355301*). The reaction was carried out in 10 mL glass vial sealed with an aluminium/Teflon[®] crimp top, which can be exposed to a maximum of $250\text{ }^\circ\text{C}$ and 20 bar internal pressure. The UV-Vis spectra were measured using a Jasco V-730 spectrophotometer. Fluorescence spectra were measured using Shimadzu make RF-5301PC spectrofluorometer. TCSPC measurements were performed by means of Horiba JobinYvon IBH having MCP PMT Hamamatsu R3809 detector instrument and all data were fitted using Data Station v2.3. Fluorescence images were captured in an Olympus iX83 fluorescence microscope with a 40X objective (Olympus) and an Andor iXon3 897 EMCCD camera in DIC, DAPI (405 nm) and FITC (488 nm) channels. A375 cell lines were purchased from National Centre for Cell Science (NCCS), Pune, India.

Section II: Optimization and experimental procedure for PJ1-PJ6

Table 1. Optimization table

Entry	Catalyst	Solvent	Time (min)	Yield*
1	MgO	1,4 dioxane	20	59
2	MgO	THF	20	57
3	MgO	EtOH	20	60
4	MgO	MeOH	20	64
5	CaO	MeOH	20	61
6	BaO	MeOH	20	70
7	BaO	1,4 dioxane	20	60
8	Ba(OH) ₂	1,4 dioxane	20	54

* Isolated yield by flash chromatography

Synthesis of sensor PJ1

Indole-3-carboxaldehyde (1.0 mmol), acetylacetone (0.5 mmol) and oven dried barium oxide (2 mmol) were suspended in dry MeOH in a 10 mL microwave glass vial equipped with a small magnetic stirring bar. The vial was tightly sealed with an aluminum/Teflon® crimp top. The closed system was then completely degassed and purged with argon for 5 min. The reaction mixture was then microwave irradiated (12 bar) for 20 min at 120 °C. After completion of the reaction, the mixture was then cooled to room temperature, filtered through a pad of celite and washed with ethyl acetate (3 × 50 mL). The filtrate was washed with water (2 × 20 mL) and with brine solution. The combined organic phase was dried over anhydrous sodium sulfate and evaporated *in vacuo*. The crude dried mass was further chromatographed on silicagel (100-200 mesh) using 30-35 % ethylacetate in hexane to furnish 218 mg of 1,5-di(3-indolyl)penta-1,4-dien-3-one (PJ1) as yellow amorphous solid (70% yield). m.p.=144-146 °C. ¹H NMR (600 MHz, DMSO-*d*₆): δ = 11.76 (s, 1H, NH), 8.11 (d, *J* = 7.2 Hz, 1H), 7.95 (d, *J* = 2.4 Hz, 1H), 7.91 (d, *J* = 15.6 Hz, 1H), 7.52 (d, *J* = 6.6 Hz, 1H), 7.22–7.18 (m, 3H). ¹³C NMR (150 MHz, DMSO-*d*₆): δ = 188.68, 138.52, 136.93, 133.44, 126.05, 123.55, 122.27, 121.83, 121.60, 113.82, 113.35. IR (KBr): $\tilde{\nu}$ = 3414, 2925.98, 1602.11, 1427.50, 1360.99, 1242.87, 1101.77, 1076.27, 742.74, 583.23 cm⁻¹. HRMS (ESI) *m/z*: calc. for C₂₁H₁₇N₂O [M + H]⁺313.1341, found 313.1343.

Probe PJ2 was synthesized in 63% yield (215mg) using the similar method to the synthesis of probe PJ1 but starting from 1-methyl indole 3 carboxaldehyde. m.p.=148-150 °C. ¹H NMR (400 MHz, DMSO-*d*₆): δ = 8.14 (d, *J* = 7.2 Hz, 1H), 7.95 (s, 1H), 7.89 (d, *J* = 16 Hz, 1H), 7.53 (d, *J* = 7.2 Hz, 1H), 7.30–7.19 (m, 3H), 3.83 (s, 3H). ¹³C NMR (100 MHz, DMSO-*d*₆): δ = 188.06, 138.53, 136.41, 135.81, 126.02, 123.16, 121.82, 121.60,

121.24, 112.37, 111.25, 33.45. HRMS (ESI) m/z: calc. for $C_{23}H_{21}N_2O$ $[M + H]^+$ 341.1654, found 341.1652.

Probe PJ3 was synthesized in 59% yield (219 mg) using the similar method to the synthesis of probe PJ1 but starting from 5-methoxy indole 3 carboxaldehyde. m.p.=152-155 °C. 1H NMR (400 MHz, Acetonitrile- d_3): δ = 9.70 (brs s, 1H, NH), 7.97 (d, J = 15.6 Hz, 1H), 7.71 (d, J = 2.8 Hz, 1H), 7.50 (d, J = 2.4 Hz, 1H), 7.41 (d, J = 8.8 Hz, 1H), 7.15 (d, J = 16 Hz, 1H), 6.91 (dd, J = 8.8 Hz, 2.4 Hz 1H), 3.91 (s, 3H). ^{13}C NMR (100 MHz, DMSO- d_6): δ = 189.28, 156.34, 136.52, 133.36, 132.11, 127.02, 122.34, 114.10, 113.86, 113.51, 103.51, 56.38. HRMS (ESI) m/z: calc. for $C_{23}H_{21}N_2O_3$ $[M + H]^+$ 373.1552, found 373.1555.

ProbePJ4 was synthesized in 64% yield (297mg) using the similar method to the synthesis of probe PJ1 but starting from 2-phenyl indole 3 carboxaldehyde. m.p.=160-164 °C. 1H NMR (400 MHz, DMSO- d_6): δ = 12.11 (s, 1H, NH), 8.20 (d, J = 7.2 Hz, 1H), 7.89 (d, J = 15.6 Hz, 1H), 7.64–7.48 (m, 6H), 7.36 (d, J = 15.6 Hz, 1H), 7.30–7.24 (m, 2H). ^{13}C NMR (100 MHz, DMSO- d_6): δ = 188.11, 144.50, 137.39, 135.96, 131.70, 130.12 (2C), 129.54, 129.45 (2C), 126.36, 123.61, 122.96, 121.80, 121.64, 112.65, 109.87. HRMS (ESI) m/z: calc. for $C_{33}H_{25}N_2O$ $[M + H]^+$ 465.1967, found 465.1968.

ProbePJ5 was synthesized in 62% yield (291mg) using the similar method to the synthesis of probe PJ1 but starting from 9-Ethyl- 3-carbazolecarboxaldehyde. m.p.=168-170 °C. 1H NMR (400 MHz, Chloroform- d): δ = 8.39 (s, 1H), 8.15 (d, J = 7.6 Hz, 1H), 8.02 (d, J = 16 Hz, 1H), 7.80 (d, J = 8.4 Hz, 1H), 7.51 (t, J = 7.6 Hz, 1H), 7.43 (d, J = 10.4 Hz, 2H), 7.30 (t, J = 7.6 Hz, 1H), 7.21 (d, J = 16 Hz, 1H), 4.39 (q, J = 21.2 Hz, 7.2 Hz, 1H), 1.47 (t, J = 7.2 Hz, 3H). ^{13}C NMR (100 MHz, Chloroform- d) δ 188.95, 144.18, 141.36, 140.49, 126.29, 126.26, 126.11, 123.50, 123.15, 122.92, 121.46, 120.65, 119.67, 108.90 (2C), 37.80, 13.87. HRMS (ESI) m/z: calc. for $C_{33}H_{29}N_2O$ $[M + H]^+$ 469.2280, found 469.2274.

ProbePJ6 was synthesized in 54% yield (319mg) using the similar method to the synthesis of probe PJ1 but starting from 9-Benzylcarbazole-3-carboxaldehyde. m.p.=165-170 °C. 1H NMR (400 MHz, Chloroform- d): δ = 8.36 (s, 1H), 8.15 (d, J = 8 Hz, 1H), 7.98 (d, J = 16 Hz, 1H), 7.46 (d, J = 7.6 Hz, 1H), 7.44 (t, J = 7.6 Hz, 1H), 7.38–7.27 (m, 4H), 7.25–7.23 (m, 2H), 7.16 (d, J = 16 Hz, 1H), 7.13–7.10 (m, 2H), 5.47 (s, 2H). ^{13}C NMR (100 MHz, Chloroform- d) δ = 188.97, 144.17, 142.13, 141.27, 136.71, 128.98 (3C), 127.77, 126.62, 126.60, 126.50, 126.48 (2C), 123.68, 123.40, 123.05, 121.51, 120.71, 120.17, 46.82. HRMS (ESI) m/z: calc. for $C_{43}H_{33}N_2O$ $[M + H]^+$ 593.2593, found 593.2595.

Section III:Photo physical studies

Solvatochromic effects of PJ1

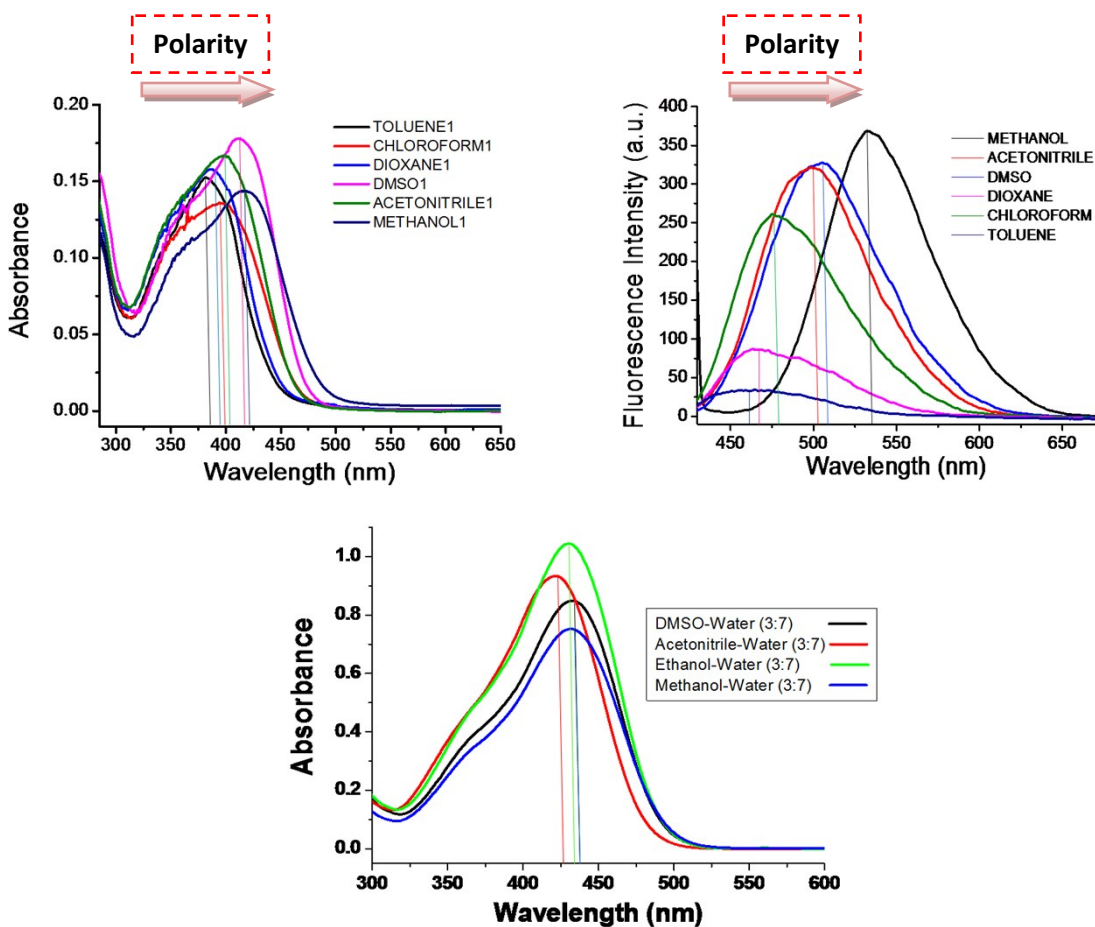
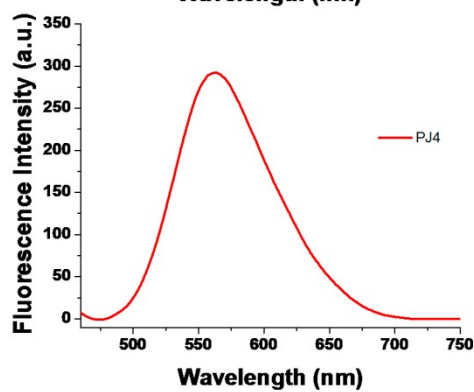
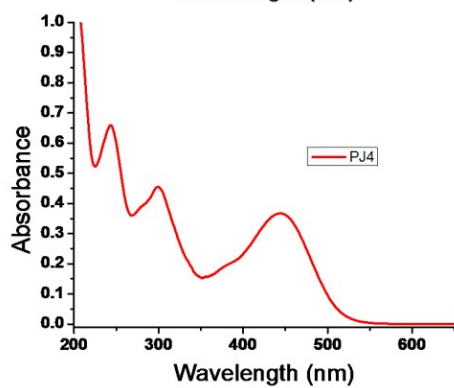
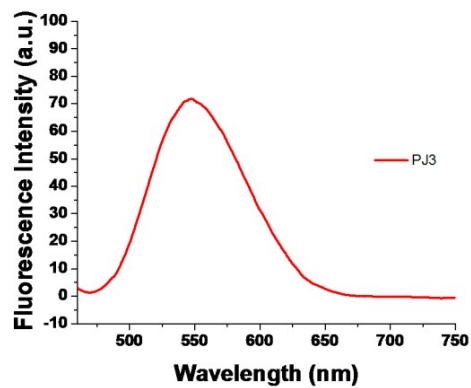
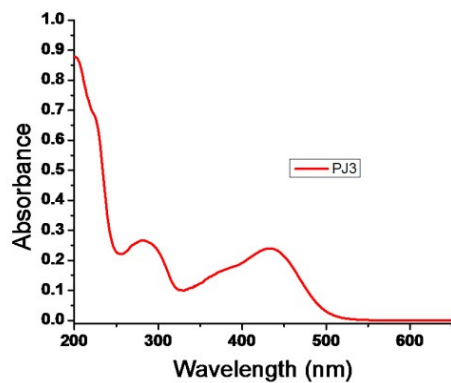
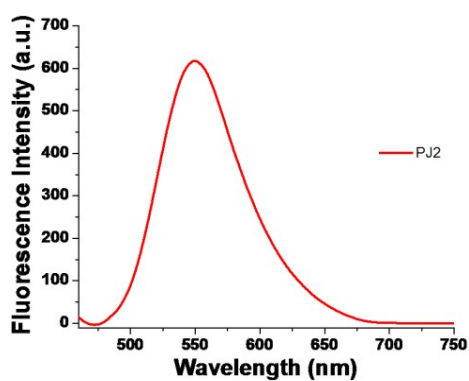
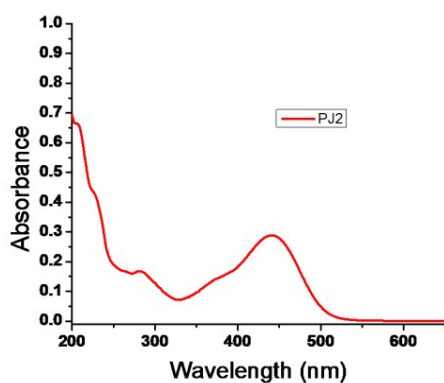
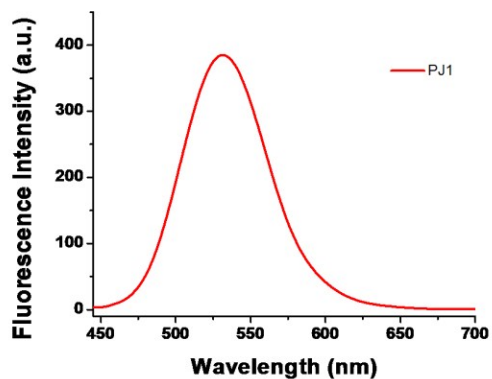
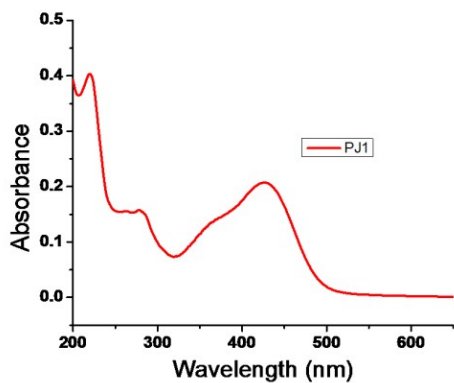


Figure 1: Solvatochromic effects of PJ1 (3.2 μM) in the following solvents: (a) Toluene, Chloroform, Dioxane, DMSO, Acetonitrile, Methanol (b) Acetonitrile-Water (3:7), DMSO-Water (3:7), Ethanol-Water (3:7), and Methanol-Water (3:7) in terms of increasing polarity.

The absorption and emission spectrum of PJ1- PJ6



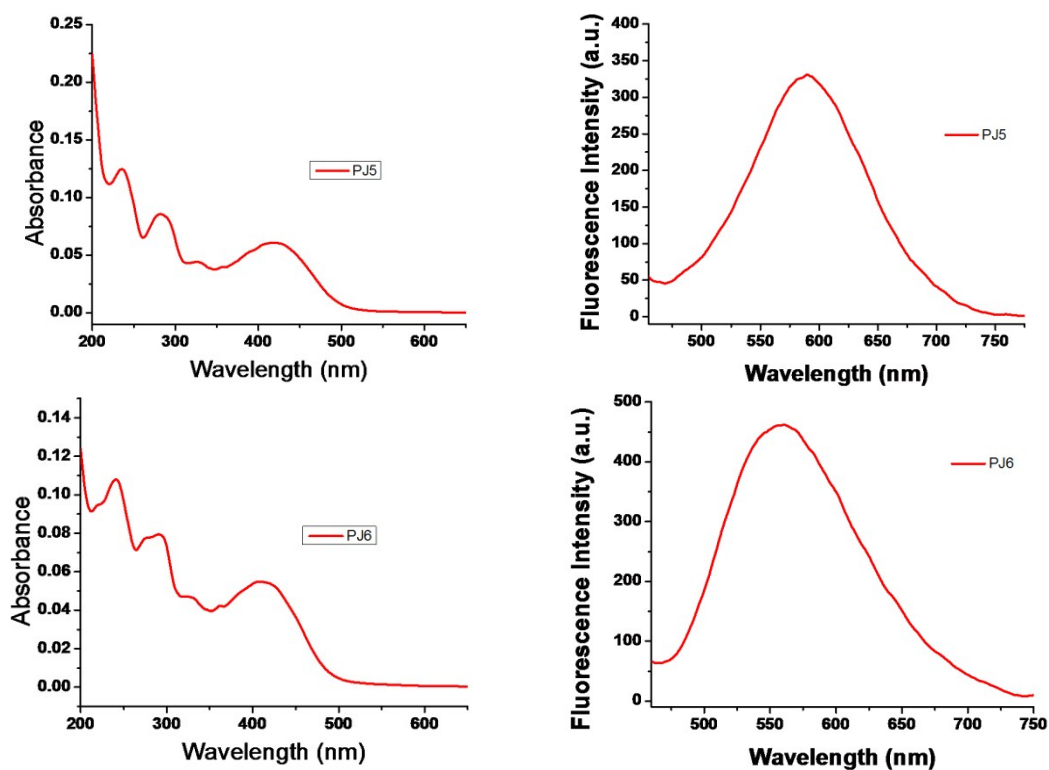


Figure 2: The absorption and emissionspectraof PJ1- PJ6 in Acetonitrile-Water (3:7)

Table 2. Stokes shifts of synthesized fluorescent C5-Curcuminoids (Acetonitrile-Water (3:7))

Entry	Compound Name	Absorption (nm) $\lambda_{\max}^{\text{ex}}$	Emission (nm) $\lambda_{\max}^{\text{em}}$	Stokes Shift(nm) $\Delta\lambda$	Stokes Shift (cm^{-1})
1	PJ1	428	536	106	4707.77
2	PJ2	445	549	104	4256.97
3	PJ3	437	547	110	4601.76
4	PJ4	446	562	116	4627.93
5	PJ5	417	590	173	7031.66
6	PJ6	410	561	151	6564.93

Section IV:Determination of detection limit

The detection limit was calculated following reported literature.¹In general, plot of $[F_0 - F_x]$ versus $[\text{Quencher}]$ was plotted, where, F_0 is the initial fluorescence intensity and F_x is the final fluorescence intensity at 536nm. Then, linear curve fitting provided the value of slope. The standard deviation of blank measurement was calculated by using three readings of blank. The detection limit was calculated using formula: $\text{LOD} = (3.3 \times \text{SD})/\text{slope}$ where, LOD= limit of

detection and SD = standard deviation of the blank (calculated by using three readings). The detection limit of homocysteine and cysteine was found to be 5.12 μM and 5.8 μM respectively.

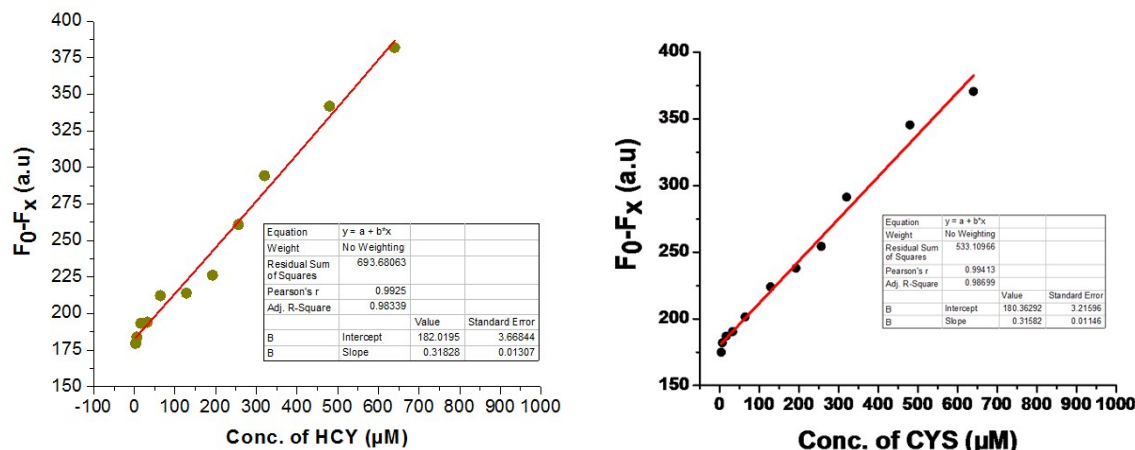


Figure 3: Linear plot of **PJ1** (3.2 μM) against (a) homocysteine (b) cysteine (0–700 μM) for calculating detection limit at 536 nm.

Section V: Kinetic study of the response of the probe PJ1 with Cys at 37 $^{\circ}\text{C}$

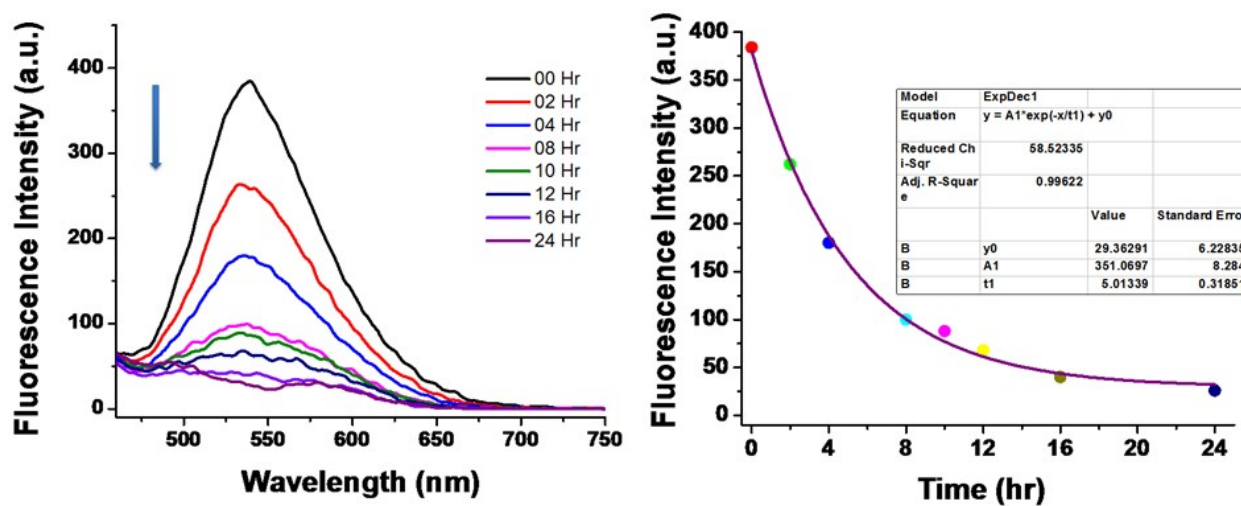


Figure 4: (a) The response of probe **PJ1** (3.2 μM) towards Cys (640 μM) with time at 37 $^{\circ}\text{C}$. (b) Exponential decrease of fluorescence intensity of probe **PJ1** in presence of Cys with time

Section VI: Determination of fluorescence quantum yield

Rhodamine-B in acetonitrile-water (3:7) (literature quantum yield in water is 0.31)¹ was chosen as the standard. The quantum yield of **PJ1** in water was calculated according to following equation:

$$\phi_F = \phi_F(\text{std}) \frac{FA_{\text{std}}\eta^2}{F_{\text{std}}A\eta_{\text{std}}^2}$$

Where ϕ_F is the quantum yield, F is the measured integrated emission intensity, η is the refractive index (1.23 for water-acetonitrile mixture), and A is the optical density. The subscript “std” refers to the reference fluorophore of known quantum yield. Quantum yield (ϕ_F) of **PJ1** was thus determined to be 0.47.

Section VII: Fluorescence lifetime measurement

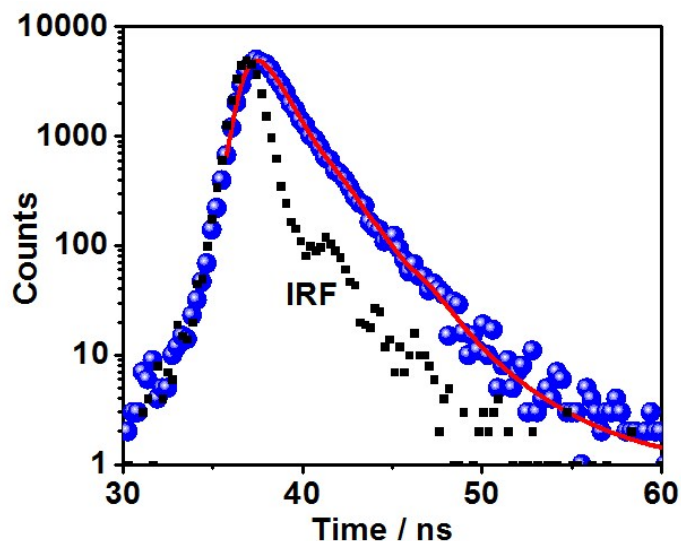


Figure 5: Representative fluorescence decay profile of probe **PJ1**

Section VIII: Fluorescence quenching at different pH

For pH dependent quenching of fluorescence intensities of **PJ1**, three different acetonitrile/ HEPES buffer (3:7) stock solutions of **PJ1** (320 μM) were prepared maintaining pH 5.0, 7.0, and 9.0 respectively. 10 μL of each stock solution were taken out, diluted 100 times with acetonitrile/ HEPES buffer (3:7) to prepare 3.20 μM experimental sample of **PJ1**. Homocysteine (200 equiv.) was added to each experimental sample and spectra were recorded at pH 5.0, 7.0, and 9.0 over time. Upon excitation of experimental samples at 428 nm, significant

decrease of fluorescence intensities over time were monitored at 536 nm emission wavelength. The titration was performed in standard quartz cuvette of 1 cm path length.

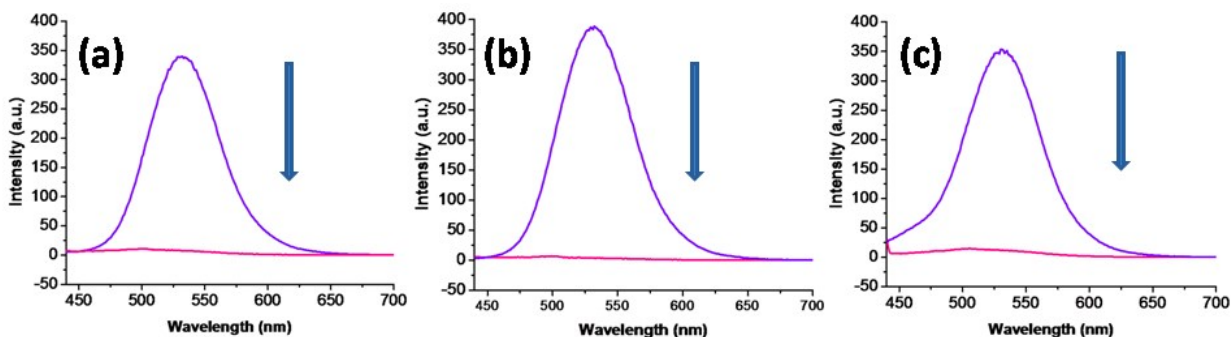


Figure 6: Fluorescence quenching of **PJ1** (3 μM) with time in presence of 200 equiv. Ofhomocysteine at pH at (a) 5.0, (b) 7.0, and (c) 9.0. at 37 °C within 24 hours

Section IX: Photostability of PJ1 vs PJ5

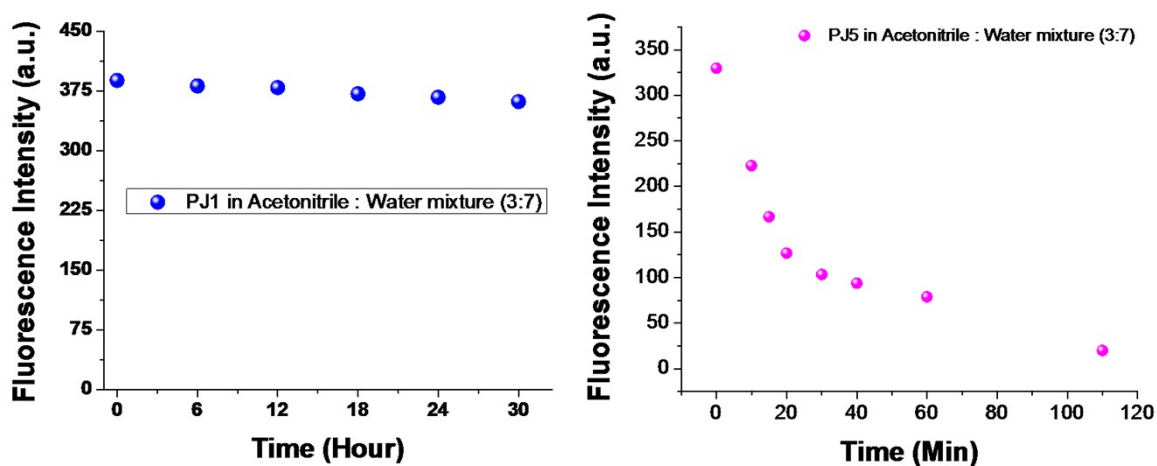


Figure 7: Photostability of **PJ1** vs **PJ5**

Section X: Kinetics of sensing of PJ1 studied by HPLC

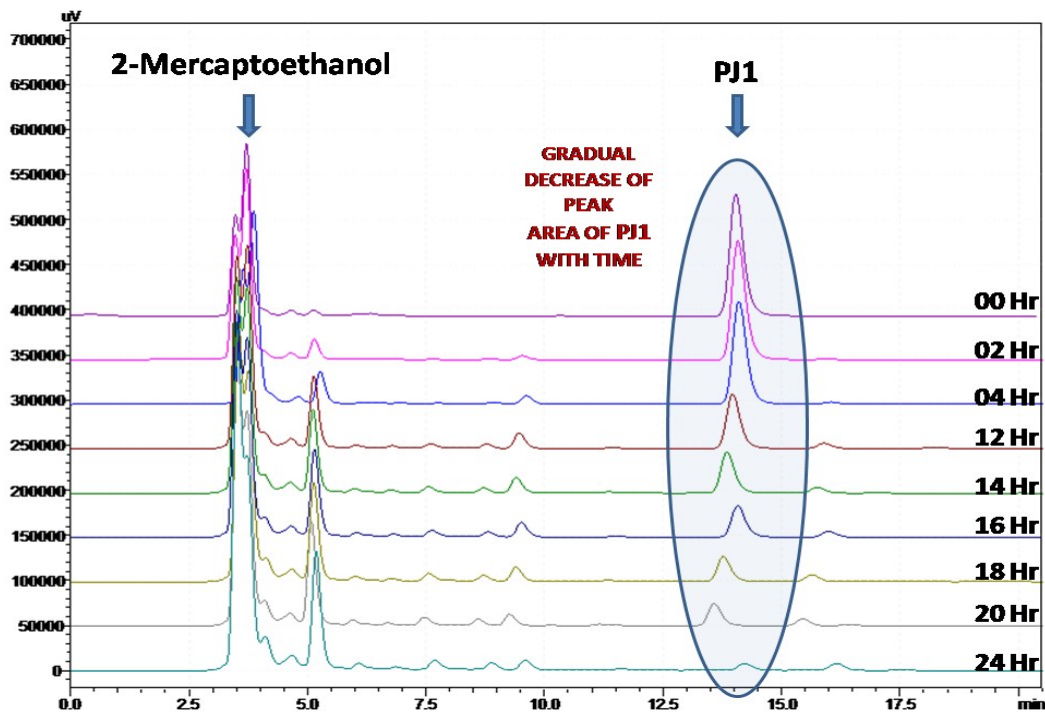


Figure 8 :HPLC profiles for decrease of probe content with time at 37 °C in 2 mercaptoethanol enriched sample.

Section XI: Procedure for cell culture and fluorescence imaging

A375 cells were seeded in a confocal dish before 24h of treatment. Cells were treated with 20 μM solution of **PJ1** in complete media for 4h. Cells were washed by media and incubated with Hoechst 33258 for 60 min. before imaging. Live cell images were taken after 6h, 12h and 24h of treatment.

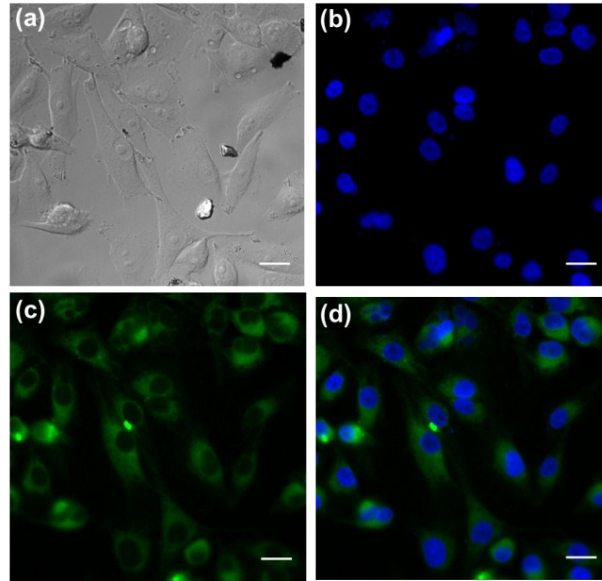


Figure 9: Fluorescence microscopic images of **PJ1** after 6h incubation in A375 cell in (a) bright field, (b) 405 nm channel, (c) 488 nm channel, and (d)merged image. Scale bars correspond to 20 μm .

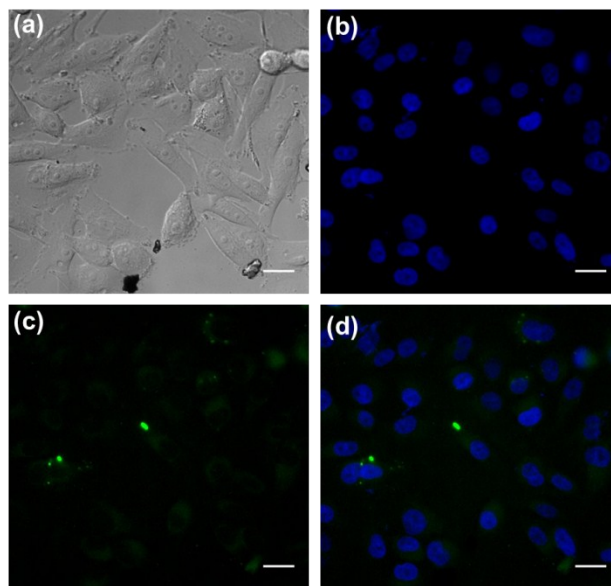


Figure 10: Fluorescence microscopic images of **PJ1** after 12 h incubation in A375 cell in (a) bright field, (b) 405 nm channel, (c) 488 nm channel, and (d)merged image. Scale bars correspond to 20 μm .

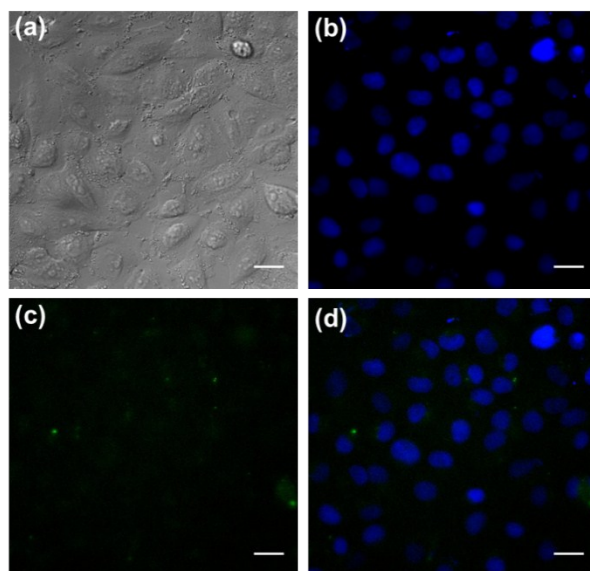


Figure 11: Fluorescence microscopic images of **PJ1** after 24 h incubation in A375 cell in (a) bright field, (b) 405 nm channel, (c) 488 nm channel, and (d) merged image. Scale bars correspond to 20 μm .

Dual acridine orange/ethidium bromide (AO/EB) cocktail has been used to identify healthy cells, early and late apoptotic cells, and necrotic cells using fluorescent microscopy. The AO penetrated normal and early apoptotic cells with intact membranes, fluorescing green when bound to DNA. EB enters into cells only when the cell membranes disintegrate, during the late apoptotic and dead cells. It binds to concentrated DNA fragments or apoptotic bodies emitting orange-red fluorescence. Furthermore, dual AO/EB staining is able to detect mild DNA injuries.

The probe **PJ1**/ EtBr (DD/EB) cocktail was used to replace AO/EB cocktail for identification of healthy cells, early and late apoptotic cells, and necrotic cells using fluorescent microscopy. In order to compare the efficiency of probe **PJ1**/EB (working concentration $1\mu\text{g}/100\ \mu\text{l}$ of probe **PJ1**) with AO/EB, healthy 60% confluent AGS cells (human gastric adeno-carcinoma call line) were treated with both the cocktails independently, washed thoroughly with phosphate buffer saline (PBS) and immediately visualized under fluorescence microscope. The healthy 60% confluent AGS cells were used as a negative control group for apoptosis. The live cells stained with **PJ1**/EB were stained green, similar to the AO/EB staining. No significant apoptotic cells or changes in quantification for cellular viability were observed for both the staining protocols.

Next, the healthy AGS cells were treated with 2.5% of ethanol for 30 min and then stained the cells with both dyes (**PJ1**/EB and AO/EB) independently, washed thoroughly with PBS and visualized under fluorescence microscope. The ethanol treatments were performed as a stress inducing agent in order to develop positive control apoptotic/damaged cells groups. As compared to the quantifications of percent of healthy, early apoptotic, late apoptotic and necrotic cells, no

significant changes were observed in the cell counts. This confirms that the developed dye is as efficient as AO for studying and imaging the cell fates.

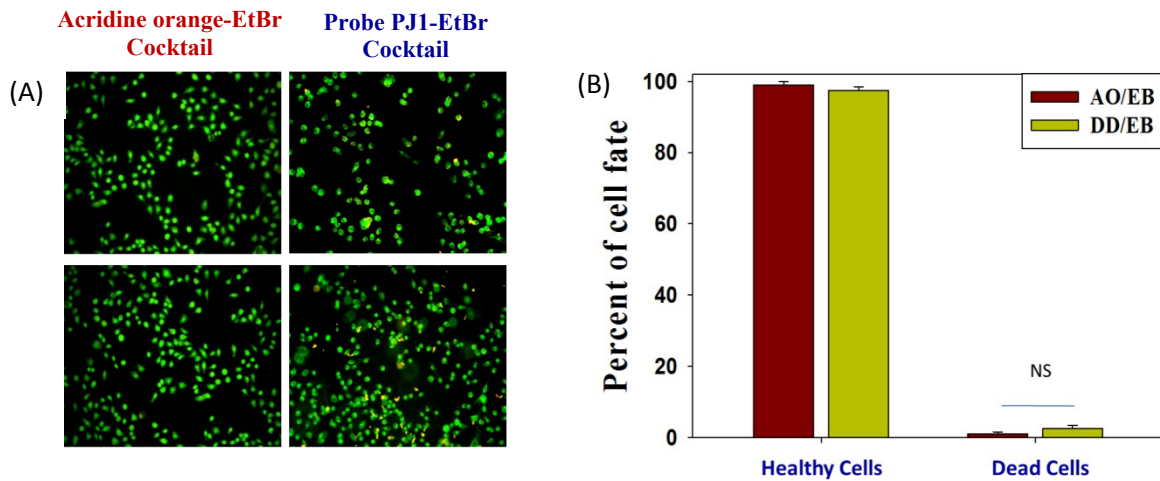


Figure 12: Comparison of DD/EB with AO/EB staining for cellular fate. (A) Healthy 60% confluent AGS cells (human gastric adeno-carcinoma cell line) were stained with both the cocktails independently, washed thoroughly with phosphate buffer saline (PBS) and visualized under fluorescence microscope. (B) Percent quantification for cell fates (for healthy and dead cells) for both staining.

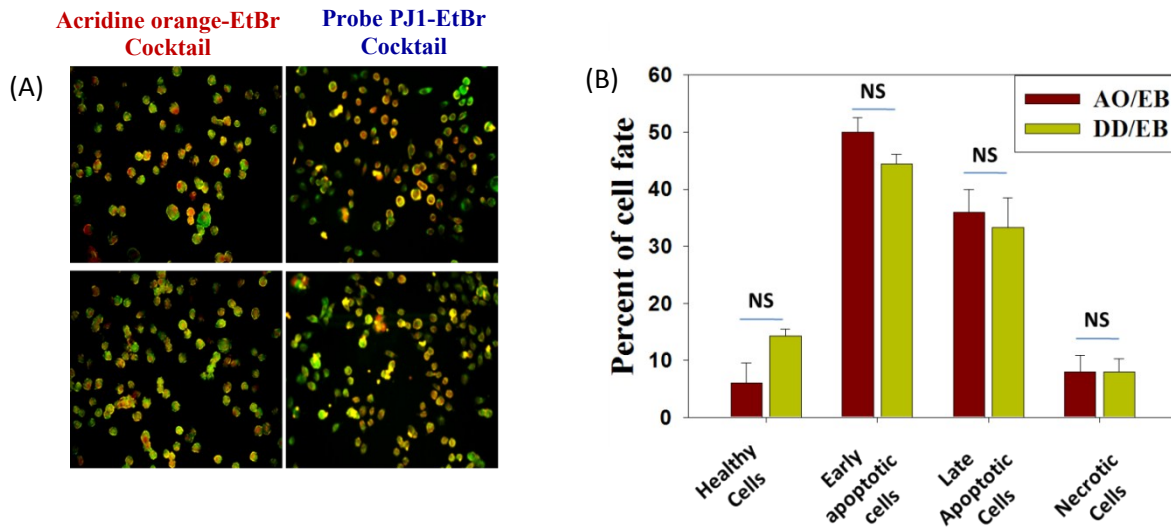


Figure 13: Comparison of Probe PJ1/EB with AO/EB staining for cellular fate. (A) Healthy 60% confluent AGS cells (human gastric adeno-carcinoma cell line) were treated with 2.5% ethanol for 30 mins and stained with both the cocktails independently, washed thoroughly with phosphate buffer saline (PBS) and immediately visualized under fluorescence microscope. (B) Percent quantification for cell fates (for healthy, apoptotic and necrotic cells) for both staining.

Section XII: ^1H NMR, ^{13}C NMR, HRMS spectra of PJ1-PJ6

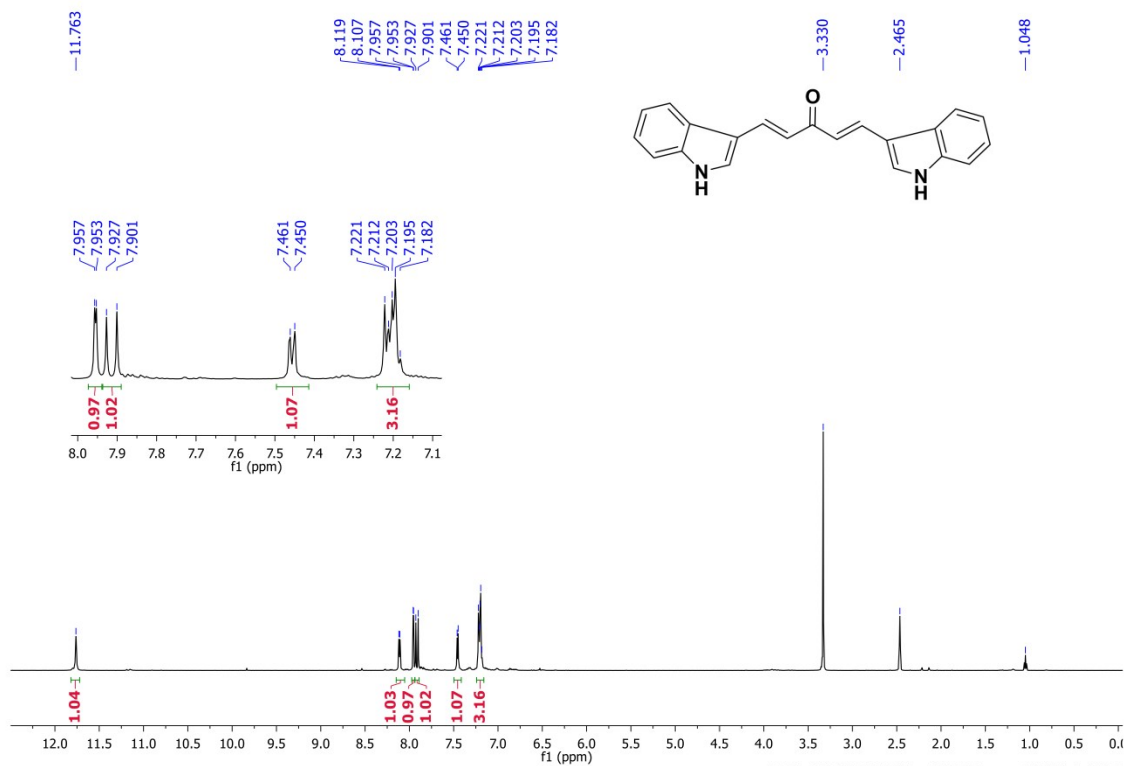


Figure 14: ^1H NMR spectrum of PJ1 in DMSO- d_6 at 600 MHz

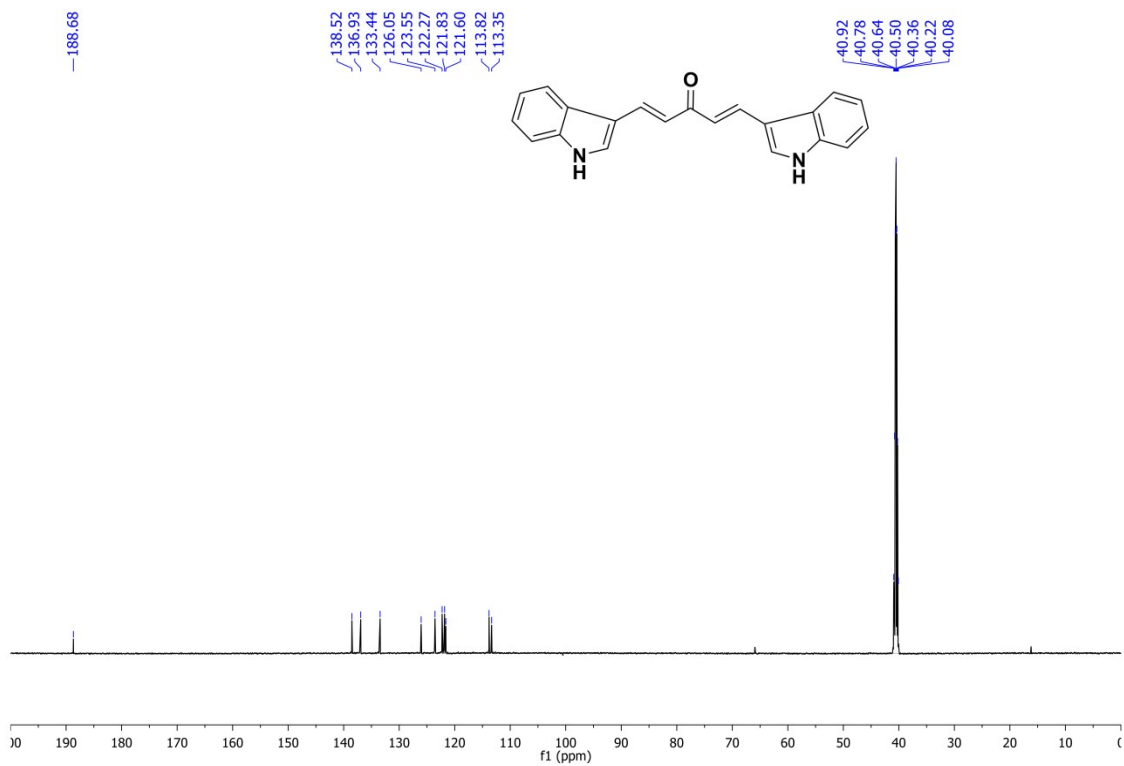


Figure 15: ^{13}C NMR spectrum of PJ1 in DMSO- d_6 at 150 MHz

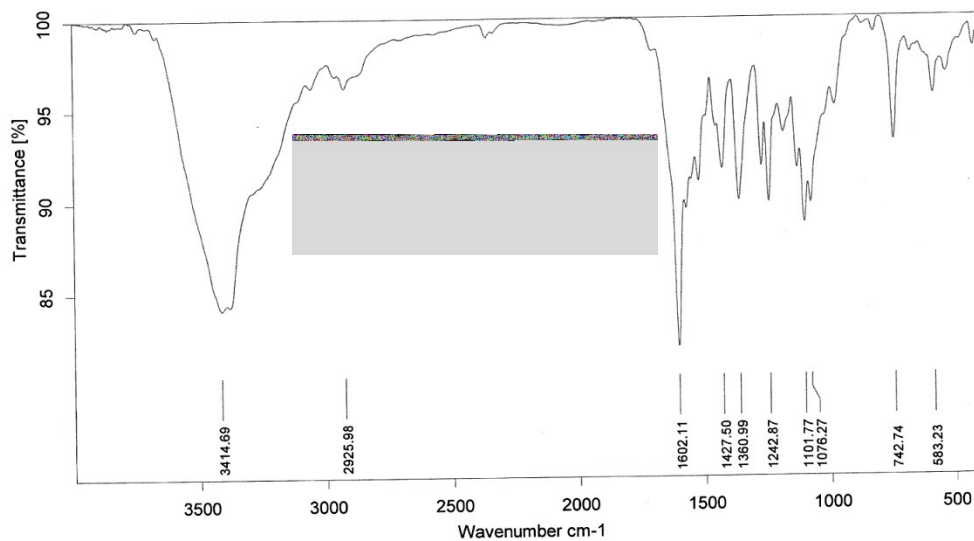


Figure 16: FT-IR spectrum of PJ1

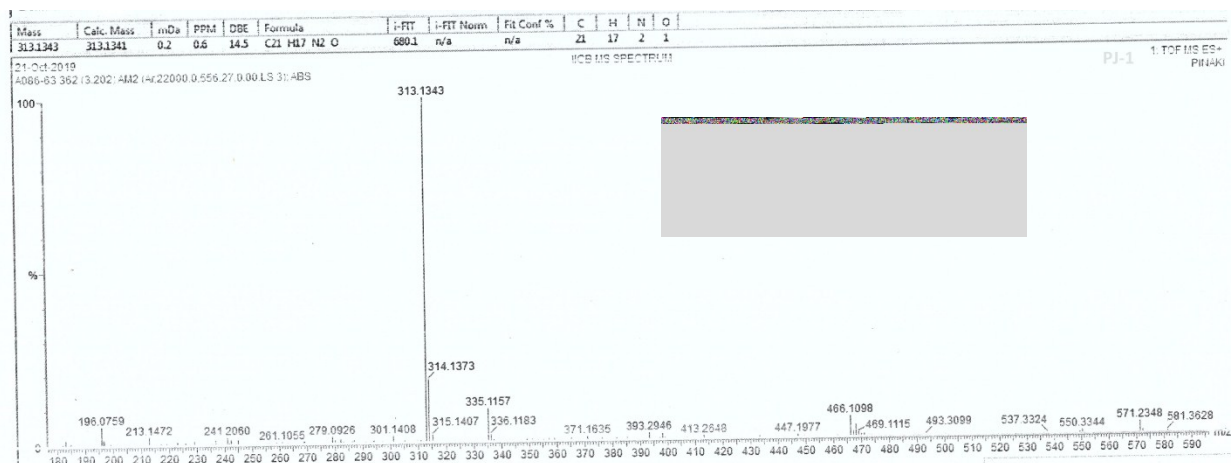


Figure 17: ESI-MS spectra of the probe PJ1

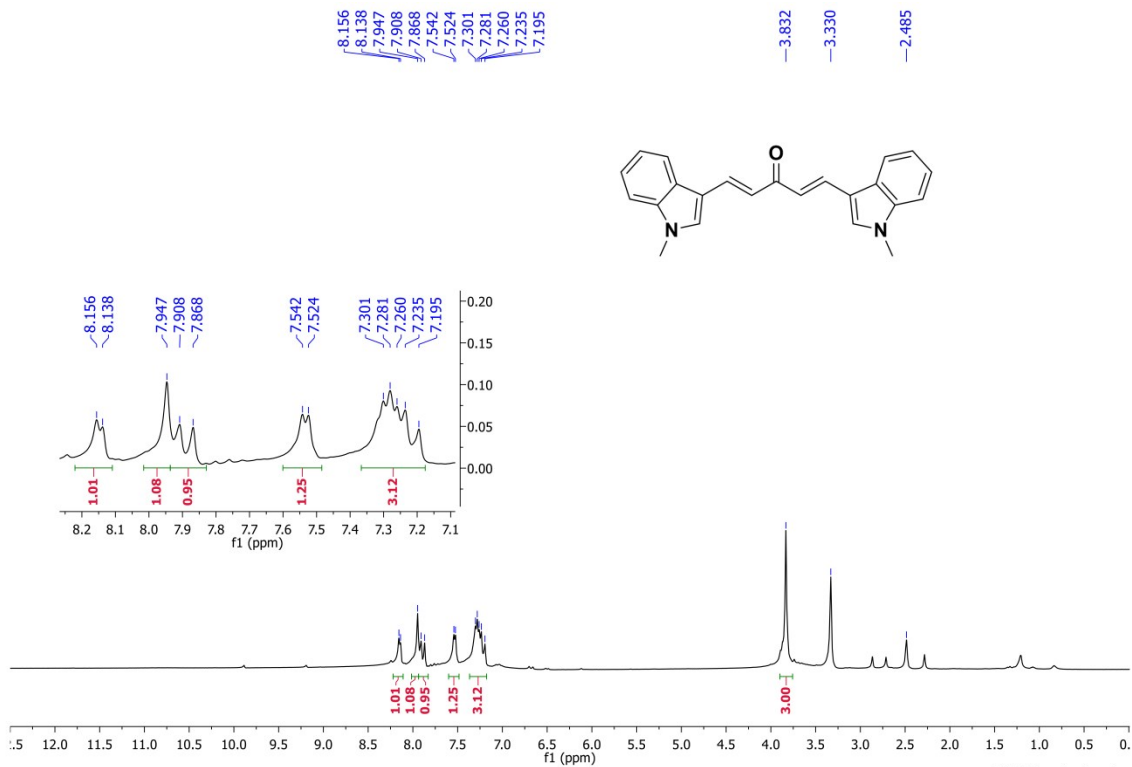


Figure 18: ¹H NMR spectrum of PJ2 in DMSO-*d*₆ at 400 MHz

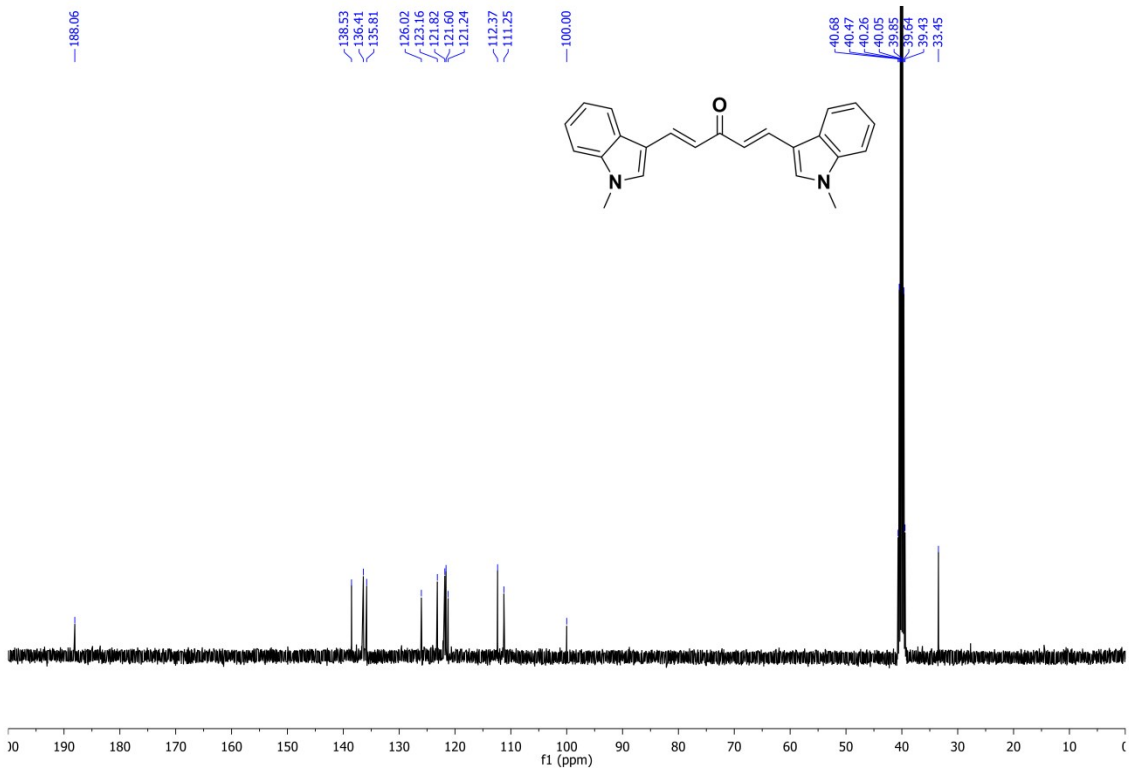


Figure 19: ¹³C NMR spectrum of PJ2 in DMSO-*d*₆ at 100 MHz

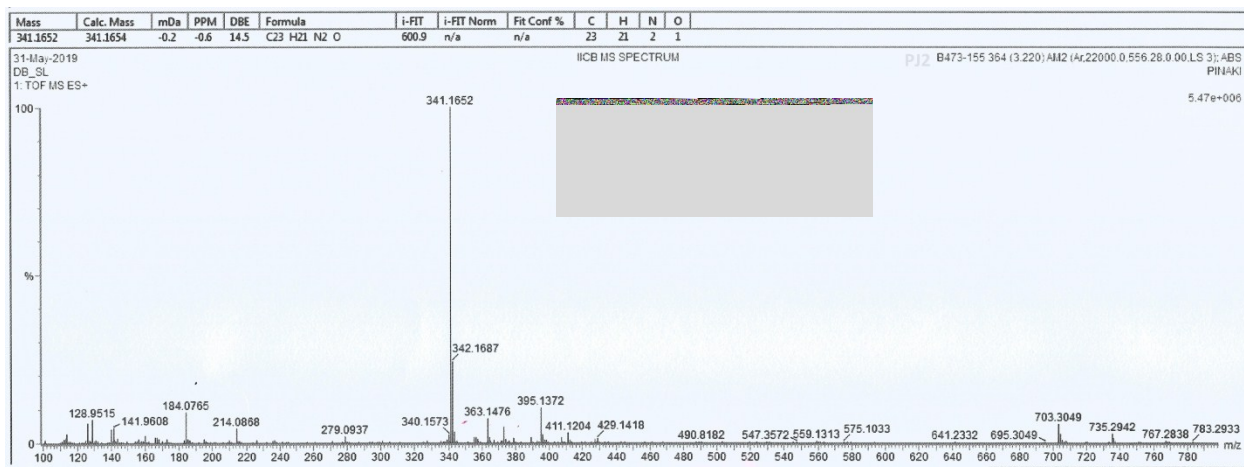


Figure 20: ESI-MS spectra of the probe PJ2

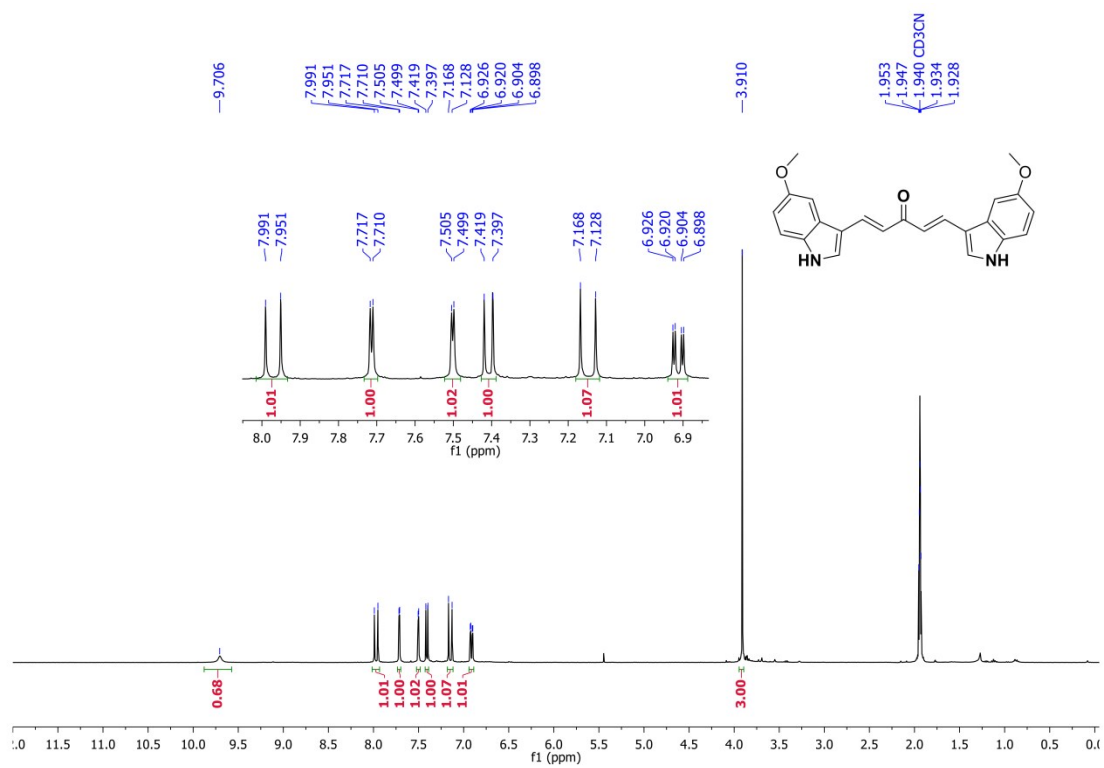


Figure 21: ¹H NMR spectrum of PJ3 in Acetonitrile-*d*₃ at 400 MHz

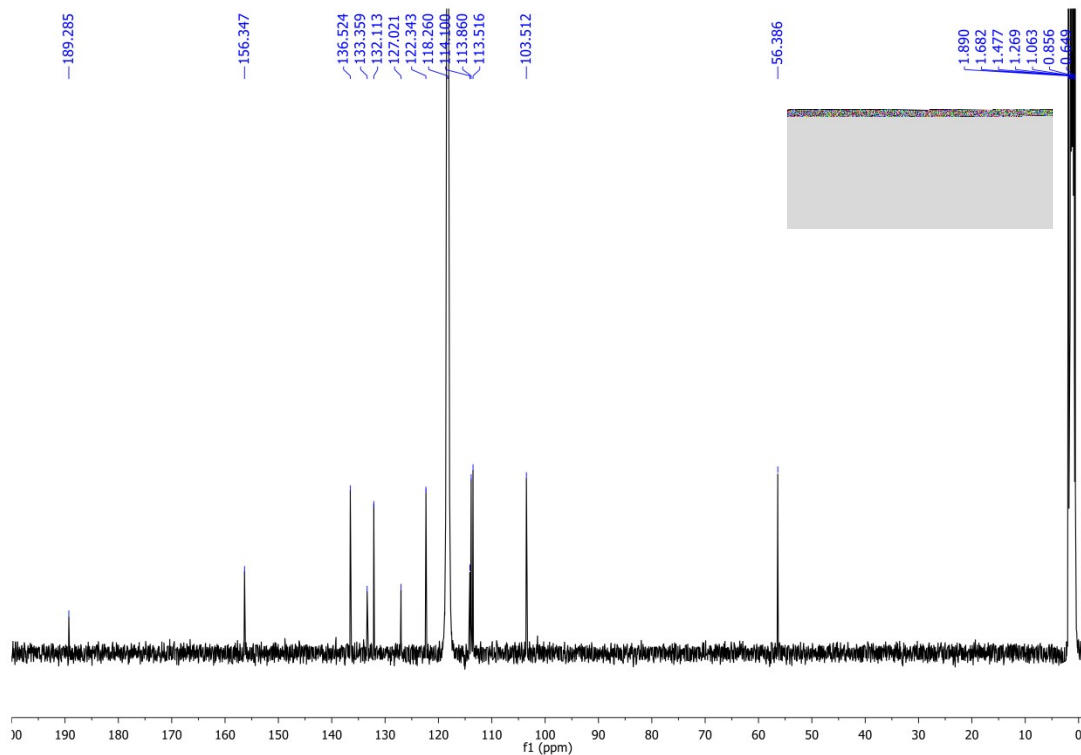
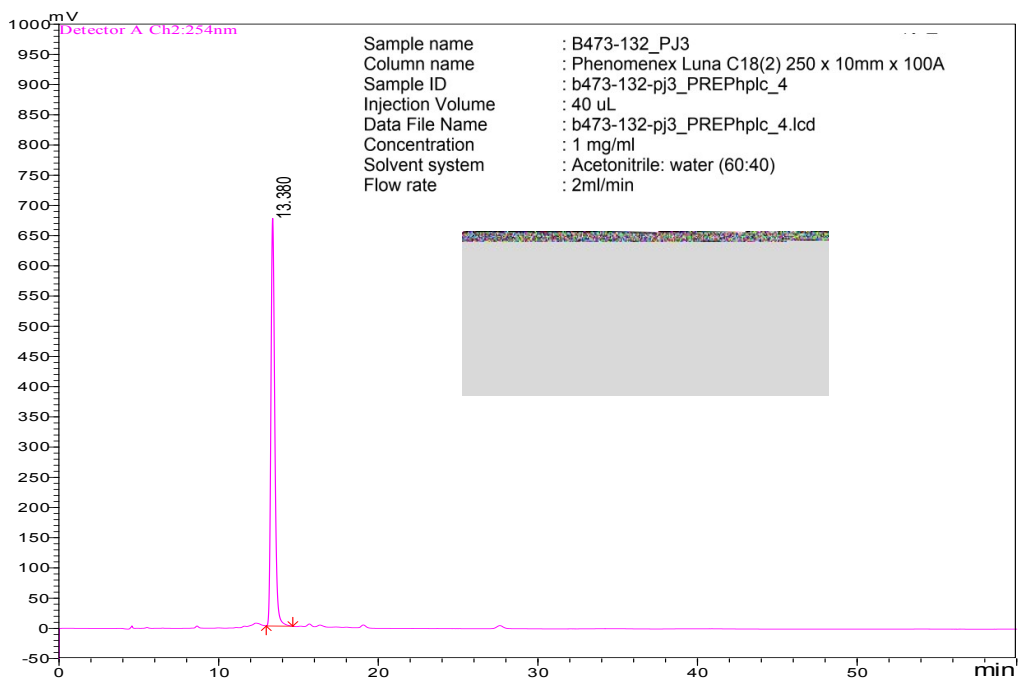


Figure 22: ^{13}C NMR spectrum of PJ3 in Acetonitrile- d_3 at 100 MHz



Sample name : B473-132_PJ3
 Column name : Phenomenex Luna C18(2) 250 x 10mm x 100A
 Sample ID : b473-132-pj3_PREPhlc_4
 Injection Volume : 40 uL
 Data File Name : b473-132-pj3_PREPhlc_4.lcd
 Concentration : 1 mg/ml
 Solvent system : Acetonitrile: water (60:40)
 Flow rate : 2ml/min

PeakTable

Detector A Ch2 254nm

Peak#	Ret. Time	Area	Height	Area %	Height %
1	13.380	11222646	673054	100.000	100.000
Total		11222646	673054	100.000	100.000

Figure 23: HPLC chromatogram of the probe **PJ3** at room temperature

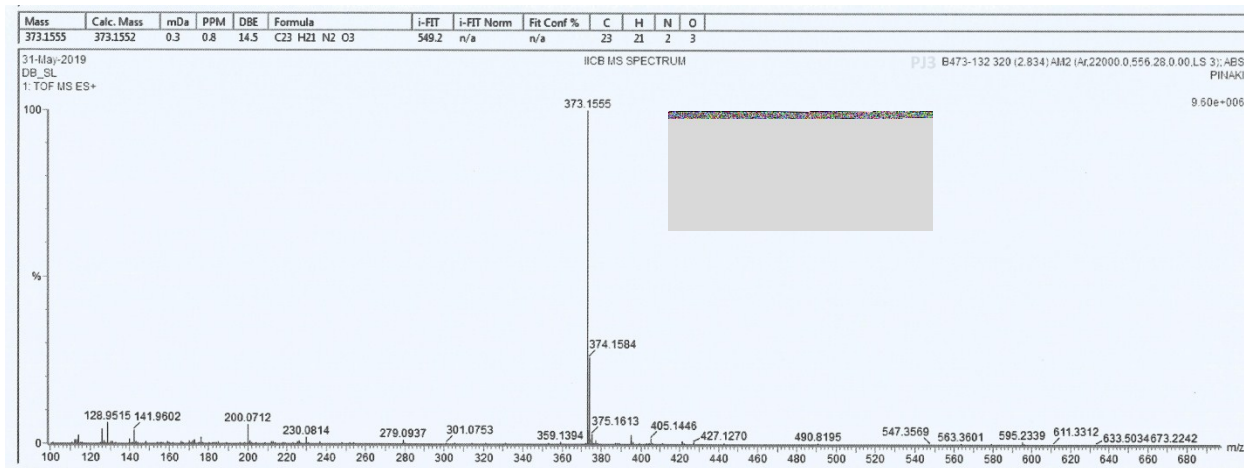


Figure 24: ESI-MS spectra of the probe **PJ3**

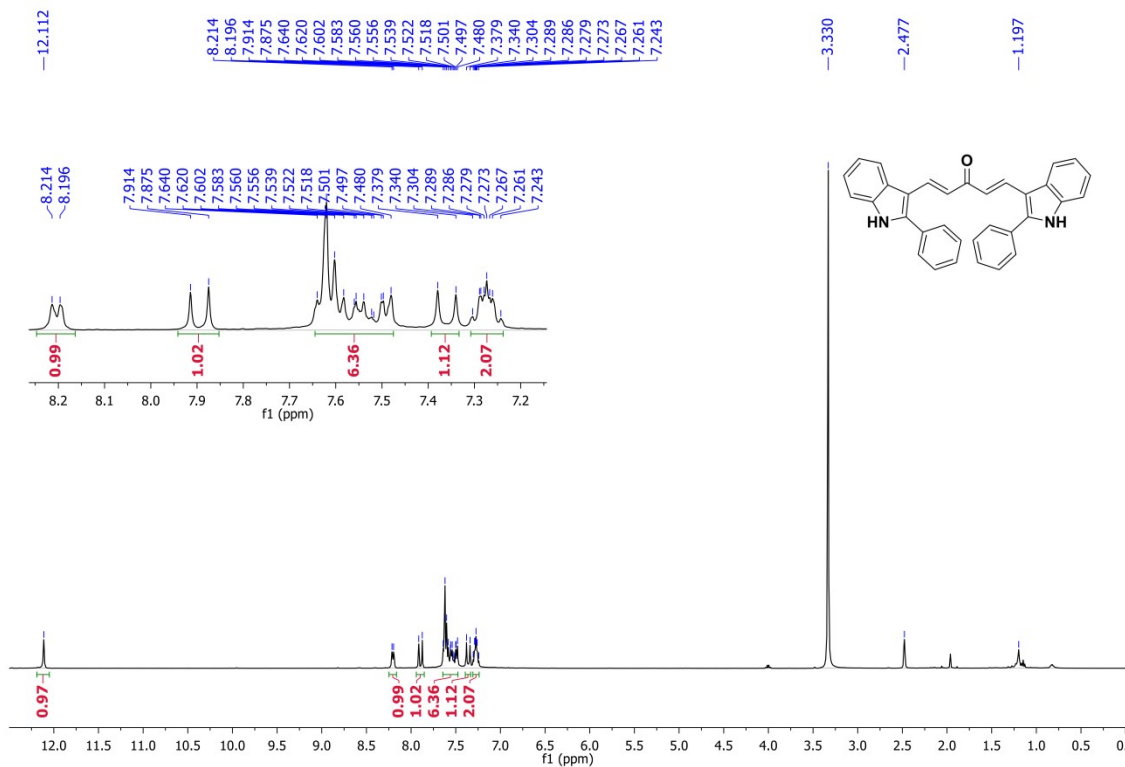


Figure 25: ^1H NMR spectrum of **PJ4** in $\text{DMSO-}d_6$ at 400 MHz

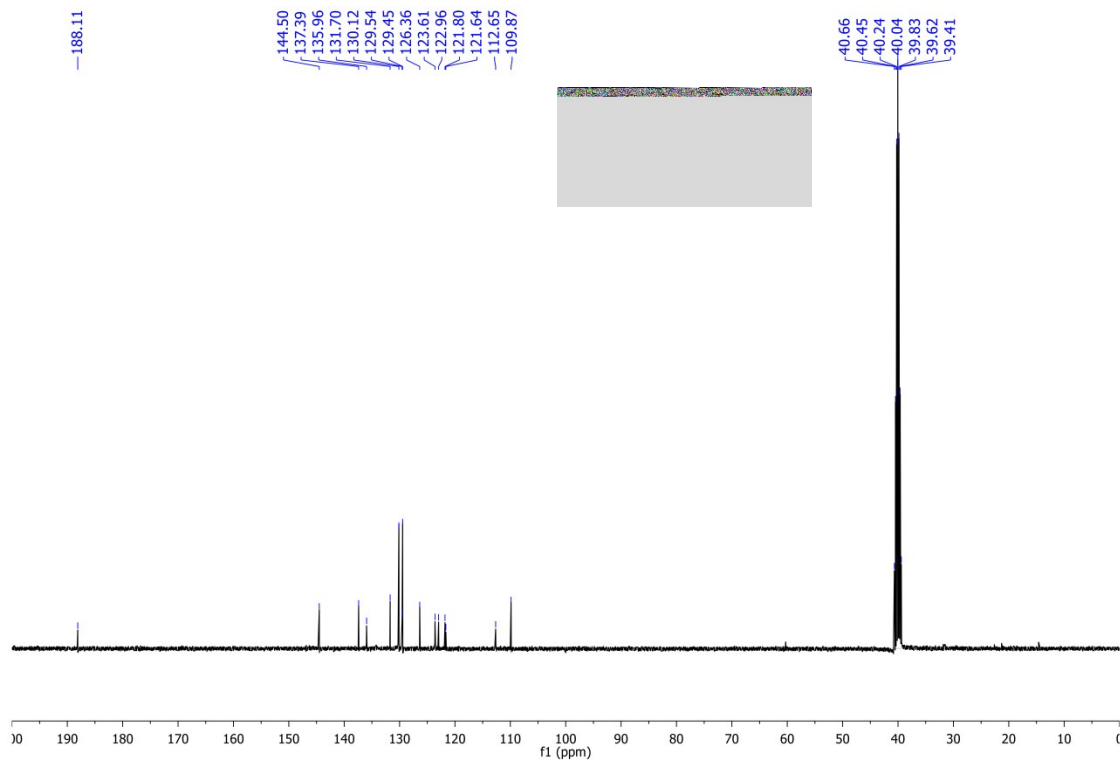


Figure 26: ^{13}C NMR spectrum of **PJ4** in $\text{DMSO-}d_6$ at 100 MHz

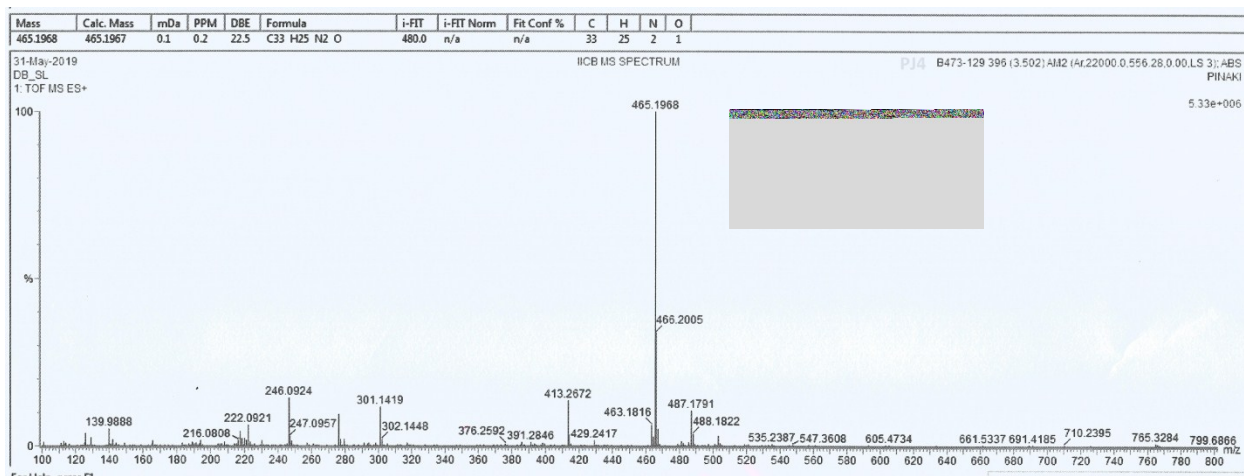


Figure 27: ESI-MS spectra of the probe **PJ4**

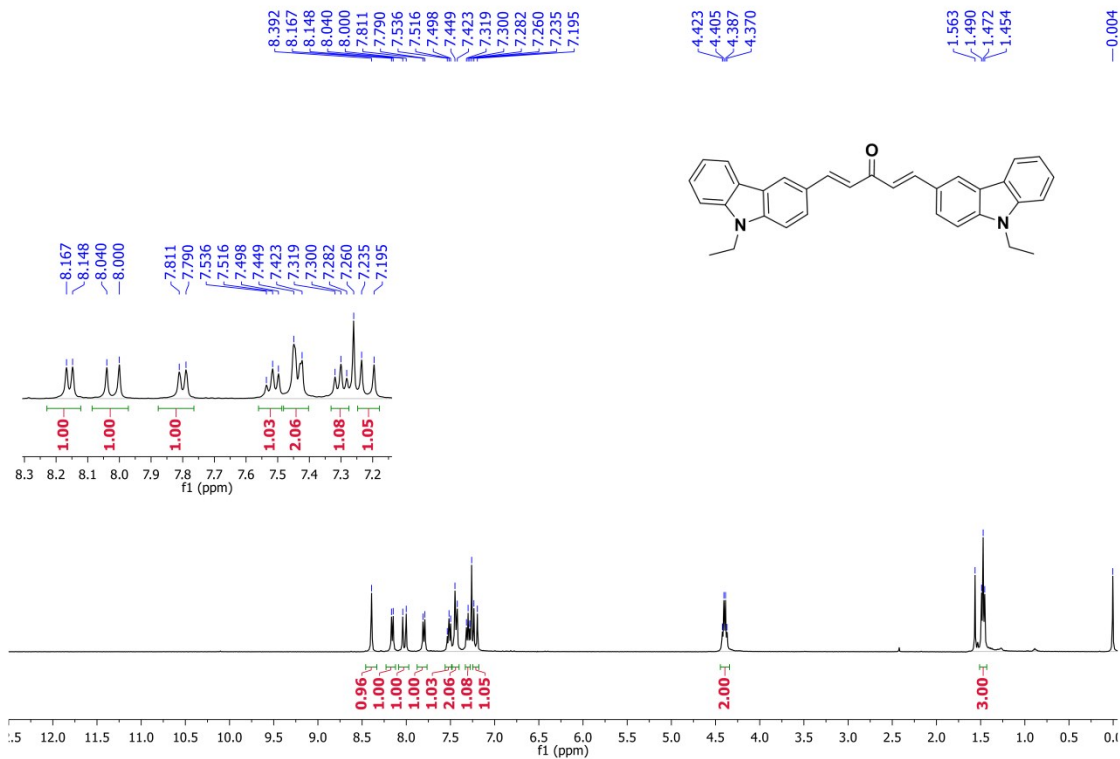


Figure 28: ^1H NMR spectrum of PJ5 in CDCl_3 at 400 MHz

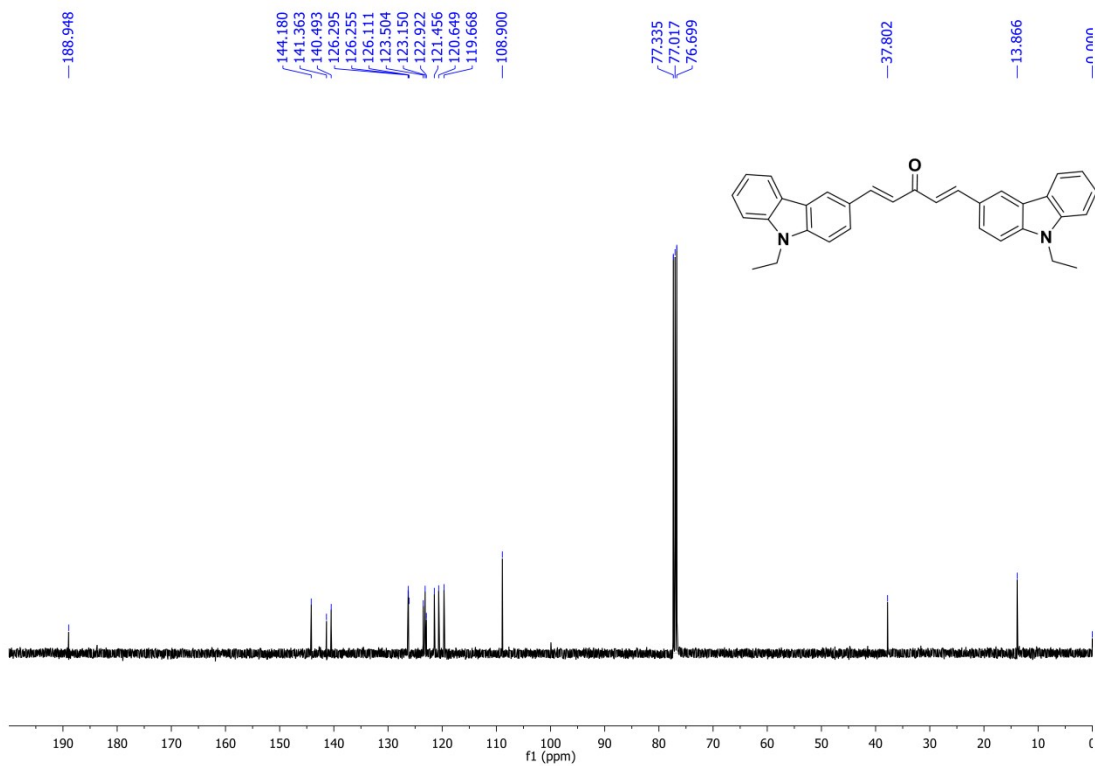


Figure 29: ^{13}C NMR spectrum of PJ5 in CDCl_3 at 100 MHz

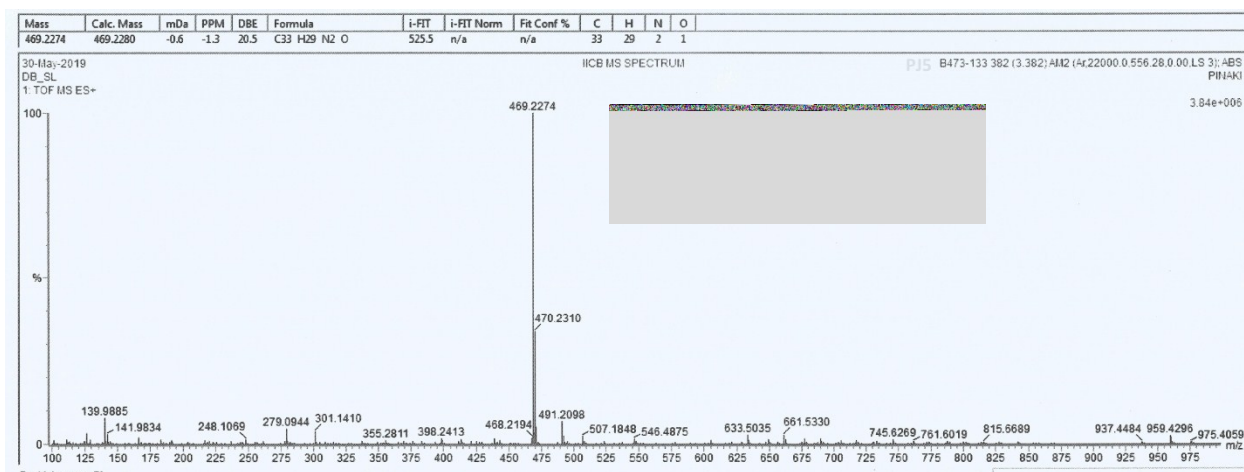


Figure 30: ESI-MS spectra of the probe **PJ5**

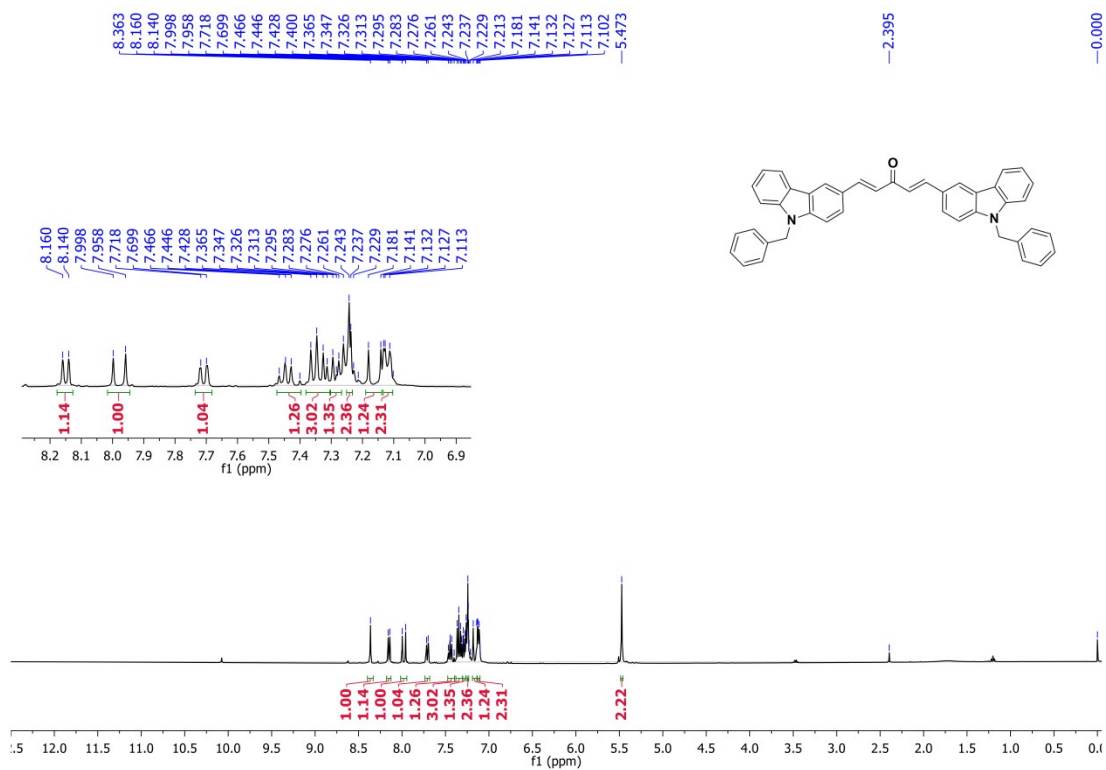


Figure 31: ^1H NMR spectrum of **PJ6** in CDCl_3 at 400 MHz

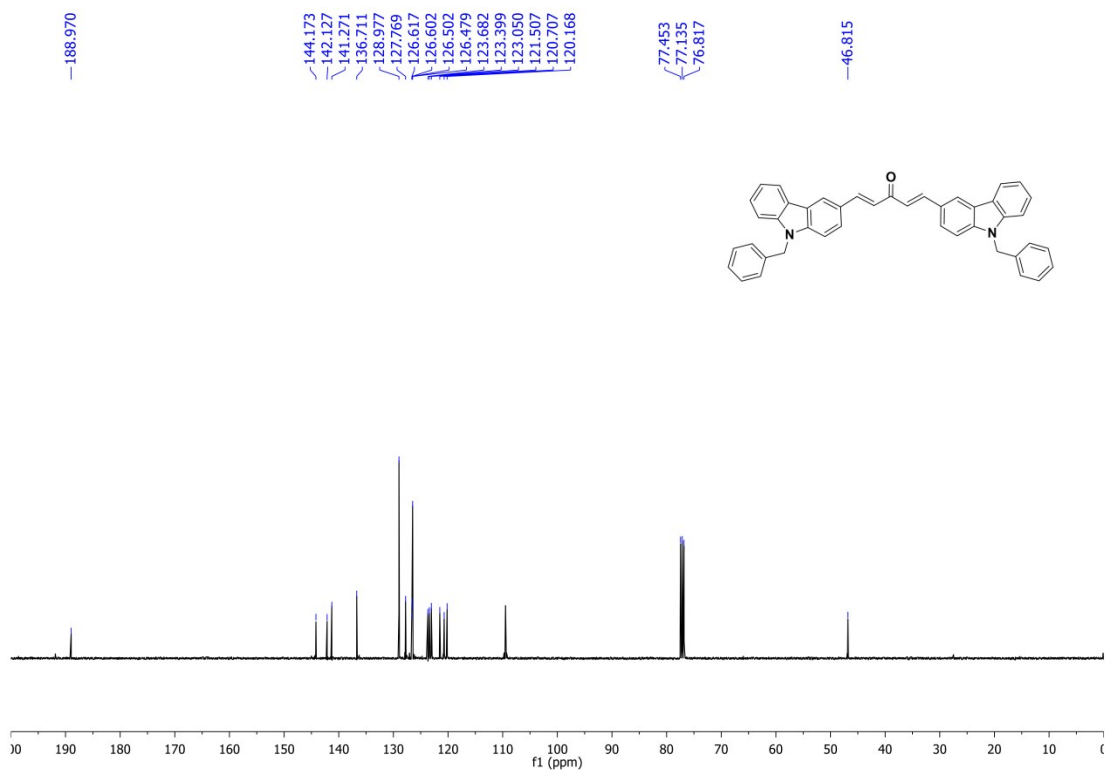


Figure 32: ^{13}C NMR spectrum of **PJ6** in CDCl_3 at 100 MHz

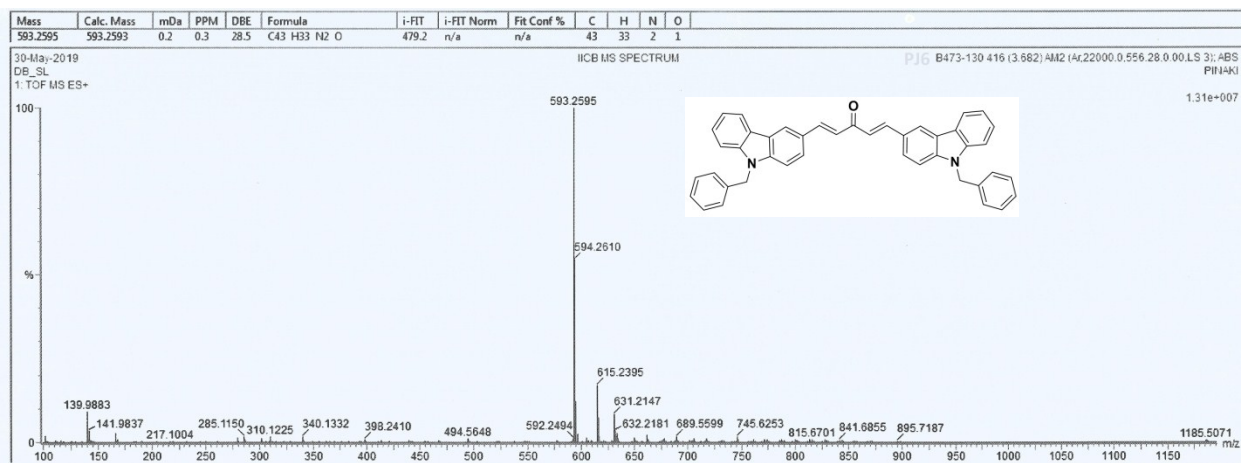


Figure 33: ESI-MS spectra of the probe **PJ6**

ESI-MS spectra of the probe-ME adduct

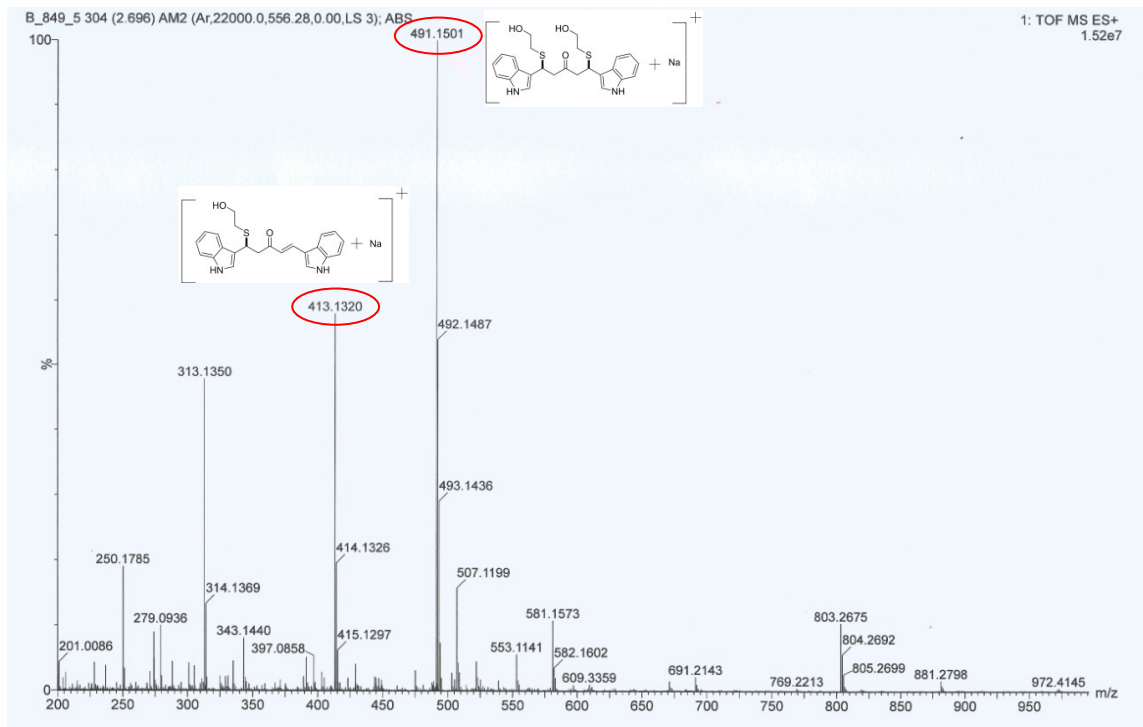


Figure 34: The ESI-MS (LCMS) spectra of product obtained by mixing Probe PJ1 with 2-mercaptoethanol (ME)

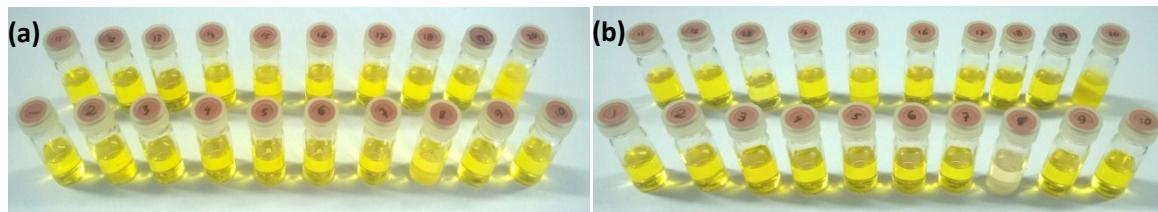


Figure 35: The color change of PJ1 solution with incubated various amino acids, observed by naked eye. (a) initially (b) after 24 hours

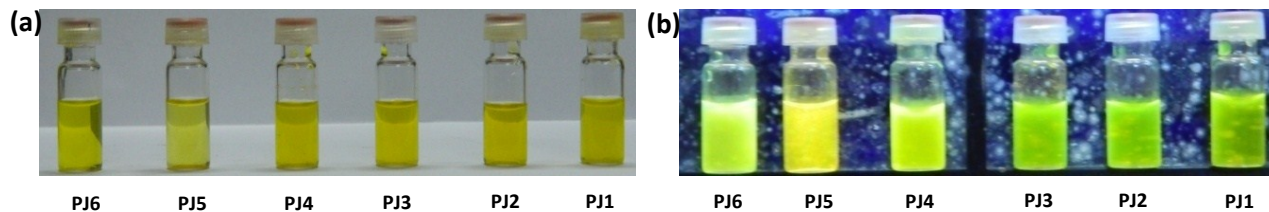


Figure 36: The color of PJ1-PJ6 solution observed by (a) naked eye (b) under 365 nm UV light

Section XI: References

1. R. Kaushik, A. Ghosh, A. Singh, P. Gupta, A. Mittal, D. A. Jose, *ACS Sens.* 2016, **1**, 1265.
2. J. Jeon, K. H. Leez, J. Rao, *Chem. Commun.*, 2012, **48**, 10034.
3. I. Shulov, S. Oncul, A. Reisch, Y. Arntz, M. Collot, Y. Mely, A. S. Klymchenko, *Nanoscale*, 2015, **7**, 18198.